

Damping of Kinetic Alfvén Eigenmodes in Tokamak Plasmas

Ph. Lauber*, S. Günter*, S.D. Pinches*, A. Könies*

*Max-Planck-Institut für Plasmaphysik, EURATOM-Association, Garching, Germany

*Max-Planck Institut für Plasmaphysik, EURATOM-Association, Greifswald, Germany

Email: pwl@ipp.mpg.de

1 Abstract

The ability to predict the stability of fast-particle-driven Alfvén eigenmodes in burning fusion plasmas requires a detailed understanding of the dissipative mechanisms that damp these modes. In order to address this question, the linear gyro-kinetic, electromagnetic code LIGKA [1] is employed to investigate their behaviour in realistic tokamak geometry. LIGKA is based on an eigenvalue formulation and self-consistently calculates the coupling of large-scale MHD modes to gyro-radius scale length kinetic Alfvén waves. It uses the drift-kinetic HAGIS code [2],[3] to accurately describe the unperturbed particle orbits in general geometry. In addition, a newly developed antenna-like version of LIGKA allows for a frequency scan, analogous to an external antenna.

With these tools the properties of the kinetically modified TAE in or near the gap (KTAE, radiative damping or ‘tunnelling’) and its coupling to the continuum close to the edge are numerically analysed. The results are compared with previous calculations based on fluid and other gyro-kinetic models. Also first linear calculations on cascade modes are presented.

2 Introduction

The stability properties of the toroidal Alfvén eigenmode (TAE) [4],[5] in magnetically confined fusion plasmas are of great interest because TAEs can be driven unstable by fusion-born α -particles with dangerous consequences for the overall plasma stability and confinement [6]. In order to make predictions for an ignited plasma like ITER, the background damping mechanisms of TAEs have to be investigated carefully. These mechanisms are electron and ion Landau damping, continuum damping, collisional damping and radiative damping. The latter mechanism requires a non-perturbative description, since the MHD properties of the mode structure are modified by coupling to the kinetic Alfvén wave (KAW) [7].

In this paper numerical calculations on the kinetic properties, especially damping rates of TAEs and KTAEs using the gyro-kinetic, linear eigenvalue code LIGKA [1] are carried out. LIGKA covers all the damping mechanisms mentioned above, except collisional damping, which is assumed to be small compared to the other types of damping.

The underlying equations of LIGKA can be simplified to the ‘reduced kinetic model’ as used in [8] and [9] proofing their validity in the regime under investigation.

3 Basics, Equations and Numerical Model

The inclusion of non-ideal effects, namely parallel electric fields and finite ion gyro-radii, leads to significant changes of the TAE modes and generates a new set of modes, the kinetic TAEs (KTAEs) and a new type of damping, called radiative damping or ‘tunnelling’ [7, 8]. They are quantified by the non-ideal parameter

$$\lambda = \frac{4ms\varrho_i}{r_m\hat{\epsilon}^{3/2}}\sqrt{\frac{3}{4} + \frac{T_e}{T_i}} \quad (1)$$

with $\varrho_i = v_{thi}/\omega_{ci}$ being the ion gyro-radius, $v_{th} = \sqrt{T/m}$ the particles’ thermal velocity, ω_c the cyclotron frequency and $\hat{\epsilon}^{3/2} = 5r_m/2R$.

In the framework of the ‘reduced kinetic model’, the following basic equation is found as the relevant one for non-ideal shear Alfvén modes:

$$\nabla_{\perp} \cdot \frac{\omega^2}{v_A^2} \nabla_{\perp} \phi + \frac{\partial}{\partial s} \nabla_{\perp}^2 \frac{\partial \phi}{\partial s} = \delta_s^2 \frac{\omega}{c} \nabla_{\perp}^4 \frac{\partial A_{\parallel}}{\partial s} - \frac{3\omega^2}{4v_A^2} \varrho_i^2 \nabla_{\perp}^4 \frac{\partial A_{\parallel}}{\partial s} \quad (2)$$

It is derived from the vorticity equation with finite Larmor radius (FLR) corrections and Ohm’s law as given in Ref. [10, 11]. Here, ϕ is the electrostatic potential, $A_{\parallel} \mathbf{b}$ the magnetic vector potential, r the radial coordinate and s the coordinate along the field line. δ_s is the skin depth $\delta_s = c^2 \epsilon_0 / \omega \sigma$ with σ being the parallel complex electrical conductivity, which was chosen to be $\sigma / \epsilon_0 = i\omega_{pe}^2 / (\omega + i\nu_{eff} - k_{\parallel}^2 v_{the}^2 / \omega)$. ω_{pe} and ν_{eff} are the electron plasma frequency and the effective electron collision frequency respectively.

Near the singular layer of the ideal MHD equation (left hand side of Eq. 2), the right hand side becomes most important and it can be simplified by the substitutions $i\omega A_{\parallel} / c \rightarrow \partial \phi / \partial s$, $\partial / \partial s \rightarrow ik_{\parallel} \equiv i(n - m/q(r))/R$, $\omega^2 / \omega_A^2 \equiv \Omega^2 = \Omega_m^2 \equiv 1/4q_m^2$ to yield a coupled system of fourth-order differential equations with the right hand side reducing to

$$-r_{LT}^2 \Omega_m^2 \frac{\partial^4 \phi_m}{\partial r^4} \quad (3)$$

with

$$r_{LT}^2 = \frac{3}{4} \varrho_i^2 + \varrho_s^2 = \varrho_i^2 \left\{ \frac{3}{4} + \frac{T_e}{T_i} \left[1 + \frac{v_A^2}{v_{the}^2} \left(1 + \frac{\nu_{eff}}{|k_{\parallel}|v_A} \right) \right] \right\}. \quad (4)$$

The underlying equations of LIGKA (derived in [12, 13]) consist of the quasi-neutrality equation

$$\sum_a \left[\int d^3 \mathbf{v} J_0 f_a + \frac{e_a}{m_a} \nabla_{\perp} \frac{n_{a0}}{B^2} \nabla_{\perp} \phi(\mathbf{x}) + \frac{3e_a v_{th,a}^2 n_{a0}}{4m_a \Omega_a^4} \nabla_{\perp}^4 \phi(\mathbf{x}) \right] = 0 \quad (5)$$

and the gyro-kinetic moment equation:

$$\begin{aligned} & - \frac{\partial}{\partial t} \frac{e}{m} \nabla_{\perp} \frac{n_0}{B^2} \nabla_{\perp} \phi + \nabla A_{\parallel} \times \mathbf{b} \cdot \nabla \left(\frac{\nabla \times \mathbf{B}}{B} \right) + (\mathbf{B} \cdot \nabla) \frac{(\nabla \times \nabla \times \mathbf{A}) \cdot \mathbf{B}}{B^2} \\ & = - \sum_a e_a \int \mathbf{v}_d \cdot \nabla J_0 f_a d^3 \mathbf{v} + \frac{c}{v_{A0}^2} \frac{3v_{th,a}^2}{4\Omega_a^2} \nabla_{\perp}^4 \frac{\partial \phi(\mathbf{x})}{\partial t} + \\ & \mathbf{B} \cdot \nabla \left(\frac{4\pi e_a^2 n_{a0} v_{th,a}^2}{2Bm_a c^2 \Omega_a^2} \nabla_{\perp}^2 A_{\parallel} \right) + \mathbf{b} \times \nabla \left(\frac{2\pi e_a n_{a0} v_{th,a}^2}{B\Omega_a} \right) \cdot \nabla \nabla^2 \phi \end{aligned} \quad (6)$$

Here, \sum_a indicates the sum over different particle species with the perturbed distribution function f_a , mass m_a , charge e_a , unperturbed density n_{a0} , thermal velocity $v_{th,a} = \sqrt{T_a/m_a}$ and cyclotron frequency Ω_a . In the same simple limit as described above, carrying out the velocity space integrals and using $A_{\parallel} = c(\nabla\psi)_{\parallel}/i\omega$, these equations can be reduced to:

$$\phi - \psi = \hat{r}_{LT}^2 \nabla_{\perp}^2 \phi \quad (7)$$

and

$$\nabla_{\perp} \cdot \frac{\omega^2}{v_A^2} \nabla_{\perp} \phi + \frac{\partial}{\partial s} \nabla_{\perp}^2 \frac{\partial \psi}{\partial s} = 0 \quad (8)$$

leading, by elimination of ψ , to exactly the same fourth order equation as given above in equations (2) and (3). It should be noted however, that \hat{r}_{LT} is not the same as r_{LT} : the physics connected with parallel electric fields and collisions (Landau damping, finite banana orbit effects) would appear on the left hand side of Eq. (7) resp. right hand side of Eq. (8) originating from the exact kinetic integrals over the velocity space.

The basic version of LIGKA [1] solves equations (5), (6) and the linear gyro-kinetic equation for the perturbed distribution function f up to 2nd order in $k_{\perp} \rho_i$. Straight field line coordinates for the background quantities given by the equilibrium code HELENA [14] are chosen. LIGKA has been extended to calculate correctly the residual part of the Landau-type integrals for the case of negative growth rates, i.e. damped modes. It uses a rational interpolation scheme for the resonance denominator which allows for accurate and fast evaluation of the pole contributions without employing derivatives. Grid refinement techniques are also applied for the velocity space integration. When examining the rich spectrum around a gap, many closely spaced modes are expected. Using a Nyquist solver is cumbersome under these conditions because many poles require a high number of sample points along the integration contour. Thus an antenna-like version of LIGKA was developed: A drive vector is added to the right hand side of the homogeneous equation:

$$M(\omega) \begin{pmatrix} \phi \\ \psi \end{pmatrix} = \mathbf{d} \quad (9)$$

where \mathbf{d} is only nonzero for the last finite element at the plasma edge, prescribing a small perturbation from the outside. The eigenfunctions are found by inverting $M(\omega)$ resulting in:

$$\mathbf{I} \begin{pmatrix} \phi \\ \psi \end{pmatrix} = M(\omega)^{-1} \mathbf{d}, \quad (10)$$

and the plasma response is ‘measured’ by an integral over the eigenfunction:

$$\mathcal{R} = \sum_m \int_0^a \phi_m \phi_m^* dr \quad (11)$$

4 Benchmarks and Results on TAEs

In this section benchmarks for the three main damping mechanisms are given:

Fig. 1 shows a benchmark with the drift kinetic perturbative CAS3D-K [15] in the Tokamak limit. Based on a real JET equilibrium case (#42979, [16]) the isotope mass of the

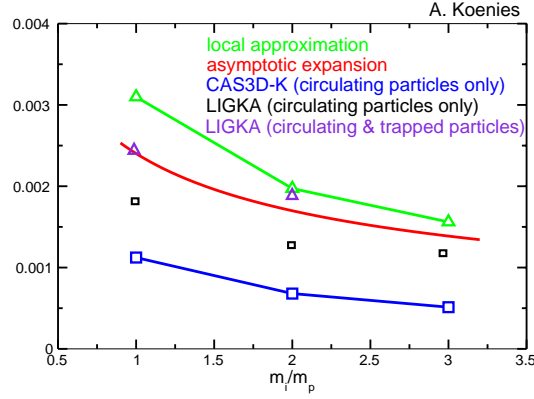


Figure 1: Damping rates for a TAE in an open gap dependent on the background isotope mass

background plasma is varied, resulting in a decreasing damping rate as the isotope mass increases. Without all the gyro-kinetic contributions, electron Landau damping is the most important damping mechanism. Agreement within a factor of 2 between the analytical calculation [17], CAS3D-K and LIGKA in the drift kinetic limit is found. However, the differences between CAS3D-K and LIGKA can be attributed to additional $E_{||}$ -effects included in LIGKA that cannot be turned off easily.

For the radiative damping, a benchmark with a code based on the reduced kinetic model[9] was carried out. For a circular equilibrium based on JET shot #38573@5.0s(details in Ref. [9]) the temperature and thus also the gyro-radius of the background ions is varied: with growing gyro-radius the non-ideal parameter λ grows, resulting in an increasing damping rate. Fig. 2 shows very good agreement between the two codes. The remaining differences may be attributed to collisional damping effects that are missing in LIGKA, but are taken into account in G. Fu’s code.

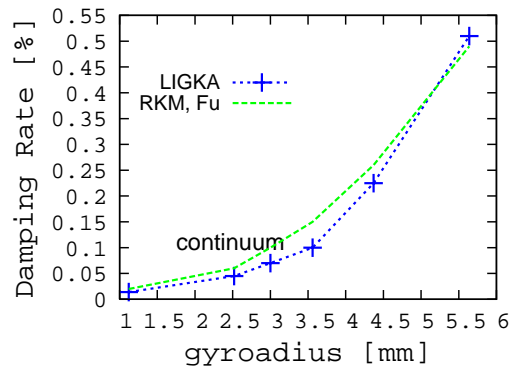


Figure 2: Dependence of the radiative damping on the gyro-radius

Figs. 3 and 4 show how the KAW 'tunnels' on top of the TAE mode: for a small gyro-radius no change in the global TAE mode structure can be seen whereas for the case corresponding to the experimental values (Fig. 3, middle) and a slightly larger gyro-radius (left) changes

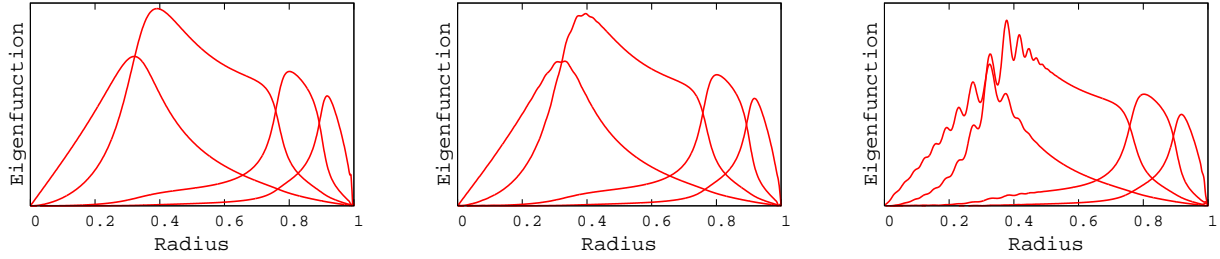


Figure 3: Eigenfunction for kinetic TAE for $\rho_i = 1\text{mm}$ (left), $\rho_i = 3\text{mm}$ (middle) and $\rho_i = 5.5\text{mm}$ (right)

in the eigenfunction can be seen. This fact confirms that a non-perturbative treatment is necessary.

The third damping mechanism, the continuum damping can be explored when the TAE gap is closed at the edge due to a small, near-zero edge density. In this case an additional KAW is excited at the modes' intersection with the Alfvén continuum as can be seen on the right in Fig. 4 at the radial position $s = 0.97$. The damping rate (LIGKA) increases to from 0.10% to 0.69%. This is relatively close to Fu's result 0.5%. Thus continuum damping at the edge is found to be the dominant damping mechanism for TAEs in a closed gap.

The calculated damping rates for an open gap are typically about a factor of 10 too small compared to experimental measurement [18][19] and other gyro-kinetic calculations [18] by PENN, [21] where mode conversion in the plasma centre was found to be the dominant damping mechanism. LIGKA finds only negligible mode conversion in the centre. However, in the closed gap case LIGKA's results become comparable to the experimental value.

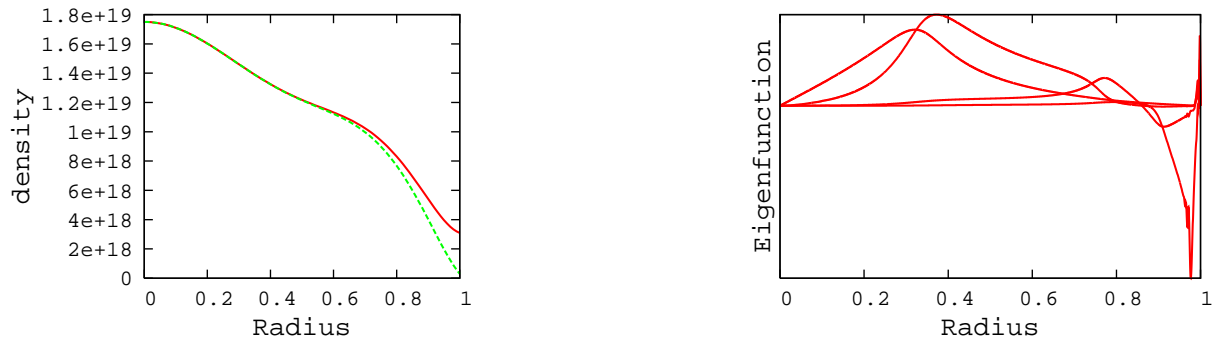


Figure 4: Density profiles for an open and closed gap case (left) and the eigenfunction for the kinetic TAE for a closed gap with $\rho_i = 3\text{mm}$ (right)

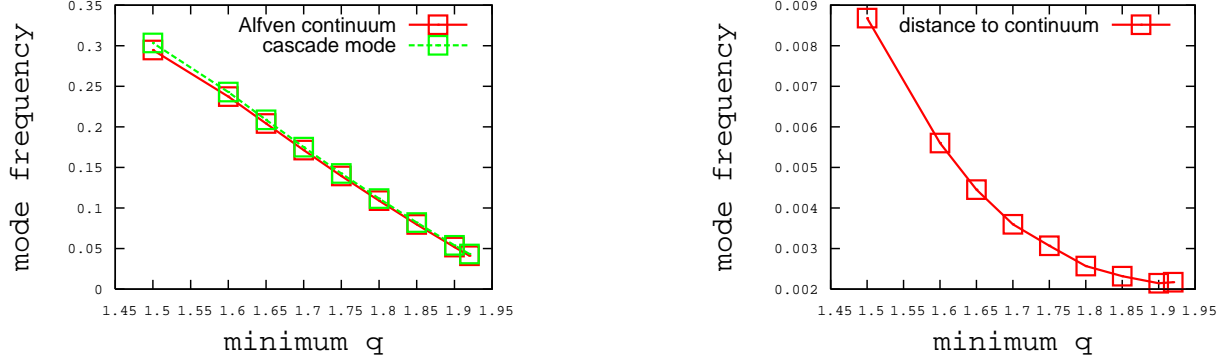


Figure 5: q_{\min} -dependence of the cascade mode frequency (left) and its distance to the Alfvén continuum (right)

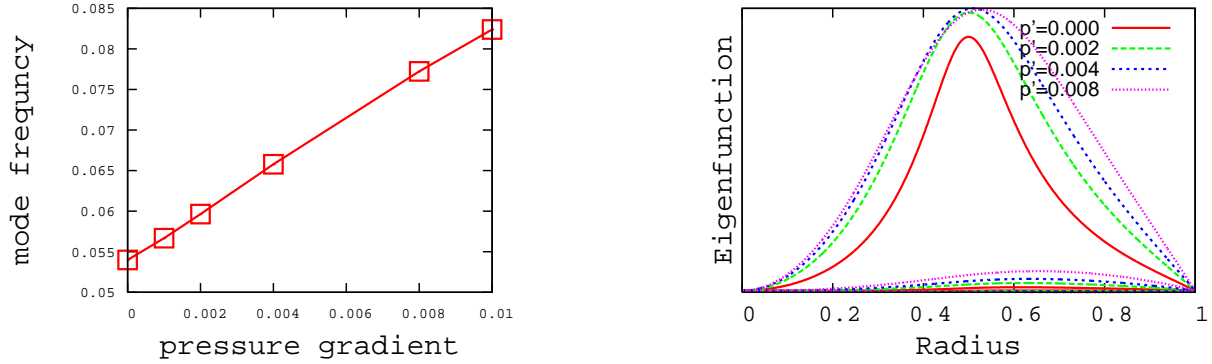


Figure 6: Dependence of the cascade mode frequency on the pressure gradient (left) and corresponding eigenfunctions (right)

5 Cascade Modes

In plasmas with a reversed q -profile global shear Alfvén modes can exist because of the lack of continuum damping near the flat shear region. There have been many experimental observations [22],[23] and also analytical analysis [24], [25]. In the latter references conditions on the existence of the mode dependent on the q -profile and mode numbers and the hot particle drive have been derived. For a shifted circle equilibrium part of these results are reproduced with LIGKA: using a parabolic q -profile with $q = q_0 + 0.5q''(s - 0.5)^2$ and ‘sweeping’ q_{\min} from $m/n = 2/1$ to $m - 0.5/n$, the mode is shifted away from the continuum [25] as shown in Fig. 5 It is also of interest how finite- β -effects modify these criteria. Numerical calculations with NOVA-K [26], CASTOR or also LIGKA in similar geometry based on numerical equilibria found that increasing the pressure gradient helps the mode to exist. A version of LIGKA for analytical equilibria in shifted circle flux geometry also confirms the numerical calculations (Fig 6). Analytical work is in progress to explain these results.

Also the non-ideal effects as continuum damping and radiative damping will be investigated.

References

- [1] Ph. Lauber, ‘Linear Gyrokinetic Description of Fast Particle Effects on the MHD Stability in Tokamaks’, Ph.D. Thesis, TU München, (2003)
- [2] S. D. Pinches, ‘Nonlinear Interaction of Fast Particles with Alfvén Waves in Tokamaks’, Ph.D. Thesis, The University of Nottingham (1996)
- [3] S. D. Pinches, L.C. Appel, J. Candy *et al.*, CPC **111**, 131 (1998)
- [4] C.Z. Cheng, L. Chen, M.S. Chance, Annals of Physics **161**, 21 (1985)
- [5] C.Z. Cheng, M.S. Chance, Phys. Fluids **29**, 11 (1986)
- [6] G.Y. Fu, J.W. VanDam, Phys. Fluids **1**, 1949 (1989)
- [7] R.R. Mett, S.M. Mahajan, Phys. Fluids B **4**, 2885 (1992)
- [8] H.L Berk, R.R. Mett, and D.M. Lindberg, Phys. Fluids B **5**, 3969 (1993)
- [9] G.Y. Fu, H. L. Berk, A. Pletzer, Phys. Plasmas **12**, 082505 (2005)
- [10] A. Hasegawa, L. Chen, Phys. Rev. Lett. **35**, 370 (1975)
- [11] A. Hasegawa, L. Chen, Phys. Fluids **19**, 1924 (1976)
- [12] H. Qin, ‘Gyrokinetic Theory and Computational Methods for Electromagnetic Perturbations in Tokamaks’, Ph.D. Thesis, Princeton University (1998)
- [13] H. Qin, W.M. Tang, G. Rewoldt, Phys. Plasmas **5**, 1035 (1998)
- [14] G.T.A. Huysmans, J.P. Goedbloed, W. Kerner, Proc. CP90 Conf. on Comp Phys. Proc., World Scientific Publ. Co., p. 371 (1991)
- [15] A. Könies, Joint Varenna-Lausanne Int. Workshop on ‘Theory of Fusion Plasmas’, (2004)
- [16] A. Jaun, private communication (2004)
- [17] G.Y. Fu, J.W. Van Dam, Phys. Fluids B **1** 2404 (1989)
- [18] A. Fasoli, A. Jaun, D. Testa, Phys. Lett. A **265**, 288 (2000)
- [19] D. Testa, G.Y. Fu, A. Jaun, A. Fasoli, O. Sauter and JET-EFDA contributors, Nucl. Fusion **43**, 479 (2003)
- [20] D. Borba, H.L. Berk, B.N. Breizman, A. Fasoli, F. Nabais, S.D. Pinches, S.E. Sharapov, D. Testa and JET-EFDA contributors, Nucl. Fusion **42**, 1029 (2002)
- [21] A. Jaun, K. Appert, J. Vaclavik and L. Villard, CPC **92**, 153 (1995)
- [22] H. Kimura *et al*, Nucl. Fusion **38**, 1303 (1998)
- [23] S.E. Sharapov *et al*, Phys. Plasmas **9**, 2027 (2002)
- [24] H.L. Berk, D.N. Borba, B.N. Breizman, S.D. Pinches, S.E. Sharapov, Phys. Rev. Lett. **87**, 185002 (2001)
- [25] B.N. Breizman, H.L. Berk, and M.S. Pekker, Phys. Plasmas **10**, 3649 (2003)
- [26] G.Y. Fu, private communication, (2005)